



## Human ex-vivo action potential model for pro-arrhythmia risk assessment



Guy Page<sup>a</sup>, Phachareeya Ratchada<sup>a</sup>, Yannick Miron<sup>a</sup>, Guido Steiner<sup>b</sup>, Andre Ghetti<sup>a</sup>, Paul E. Miller<sup>a</sup>, Jack A. Reynolds<sup>a</sup>, Ken Wang<sup>b</sup>, Andrea Greiter-Wilke<sup>b</sup>, Liudmila Polonchuk<sup>b</sup>, Martin Traebert<sup>c</sup>, Gary A. Gintant<sup>d</sup>, Najah Abi-Gerges<sup>a,\*</sup>

<sup>a</sup> AnaBios Corporation, San Diego, CA 92109, USA

<sup>b</sup> Roche Pharma Research and Early Development, Pharmaceutical Sciences, Roche Innovation Center, Basel, Switzerland

<sup>c</sup> Novartis Institutes of Biomedical Research, Safety Pharmacology, CH-4057 Basel, Switzerland

<sup>d</sup> Department of Integrative Pharmacology Integrated Sciences & Technology, AbbVie, North Chicago, IL, USA

### ARTICLE INFO

#### Article history:

Received 16 March 2016

Received in revised form 3 May 2016

Accepted 24 May 2016

Available online 25 May 2016

#### Keywords:

Human heart

Ventricular trabeculae

Action potential

Pro-arrhythmia assessment

Drug discovery and development

### ABSTRACT

While current S7B/E14 guidelines have succeeded in protecting patients from QT-prolonging drugs, the absence of a predictive paradigm identifying pro-arrhythmic risks has limited the development of valuable drug programs. We investigated if a human ex-vivo action potential (AP)-based model could provide a more predictive approach for assessing pro-arrhythmic risk in man. Human ventricular trabeculae from ethically consented organ donors were used to evaluate the effects of dofetilide, d,l-sotalol, quinidine, paracetamol and verapamil on AP duration (APD) and recognized pro-arrhythmia predictors (short-term variability of APD at 90% repolarization (STV(APD90)), triangulation (ADP90-APD30) and incidence of early afterdepolarizations at 1 and 2 Hz to quantitatively identify the pro-arrhythmic risk. Each drug was blinded and tested separately with 3 concentrations in triplicate trabeculae from 5 hearts, with one vehicle time control per heart. Electrophysiological stability of the model was not affected by sequential applications of vehicle (0.1% dimethyl sulfoxide). Paracetamol and verapamil did not significantly alter anyone of the AP parameters and were classified as devoid of pro-arrhythmic risk. Dofetilide, d,l-sotalol and quinidine exhibited an increase in the manifestation of pro-arrhythmia markers. The model provided quantitative and actionable activity flags and the relatively low total variability in tissue response allowed for the identification of pro-arrhythmic signals. Power analysis indicated that a total of 6 trabeculae derived from 2 hearts are sufficient to identify drug-induced pro-arrhythmia. Thus, the human ex-vivo AP-based model provides an integrative translational assay assisting in shaping clinical development plans that could be used in conjunction with the new CiPA-proposed approach.

© 2016 Elsevier Inc. All rights reserved.

### 1. Introduction

During the last decade pharmaceutical productivity has plummeted (Scannell, Blanckley, Boldon, & Warrington, 2012). While multiple factors have contributed to this problem, it is widely recognized that the inability to accurately and consistently predict candidate drug safety at the preclinical stage is a critical issue. More than half of all development programs are terminated due to safety-related issues, not anticipated by the preclinical studies (Cook et al., 2014). This has called into question the reliability of current preclinical safety-testing paradigms, which rely predominantly on animal models, and has led to demands for more predictive human-relevant tools (Holmes, Bonner, & Jones, 2015). Cardiotoxicity has played a major role in this 'productivity crisis'

and remains a predominant cause of drug development discontinuation and withdrawal of marketed drugs (Piccini et al., 2009).

Current strategies for the identification of pro-arrhythmic liabilities involve a combination of preclinical in vitro hERG channel assays and in vivo animal cardiovascular studies (Anon., 2005a), followed by an extensive and expensive clinical ECG-based cardiac repolarization study, known as the Thorough QT (TQT) study (Anon., 2005b), which is usually conducted in the later stages of the drug development. The TQT study is designed to characterize the potential effects of a drug candidate on ventricular repolarization in order to determine if additional cardiac monitoring is required. While TQT studies have been relatively effective in preventing approval and marketing of new drugs with strong pro-arrhythmic potential (Ewart et al., 2014; Vargas et al., 2015), the strategy has significant shortcomings. Most critically, QT prolongation has been found to be an imperfect marker for drug-related pro-arrhythmic effects (torsade-de-pointes (TdP) arrhythmia) (Anon., 2005b; Shah, 2005). In

\* Corresponding author at: 3030 Bunker Hill St., Suite 312, San Diego, CA 92109, USA.  
E-mail address: [Najah.abigerges@anabios.com](mailto:Najah.abigerges@anabios.com) (N. Abi-Gerges).

addition, the current QT-focused strategy can result in the termination of safe and effective drugs, given the documented potential for false positives (Polak, Pugsley, Stockbridge, Garnett, & Wiśniowska, 2015; Stockbridge, Morganroth, Shah, & Garnett, 2013). As a result, the FDA has initiated the evaluation of alternative strategies and new preclinical models to provide a more reliable and cost effective pro-arrhythmic safety assessment. In a collaborative effort between FDA, Cardiac Safety Research Consortium, ILSI Health and Environmental Sciences Institute, Pharmaceutical Industry and Key Opinion Leaders, a new initiative has been launched which is aimed at revising the QT paradigm and potentially eliminating the need for TQT studies. The CiPA (Comprehensive in vitro Pro-arrhythmia Assay) initiative is focused on updating the current cardiac safety testing paradigms and identifying a novel approach to better evaluate pro-arrhythmia risk, potentially removing the need for TQT studies and reducing the attrition of drugs that may benefit patients (Fermini et al., 2016; Gintant, Sager, & Stockbridge, 2016; Sager, Gintant, Turner, Pettit, & Stockbridge, 2014).

The CiPA initiative established that incremental improvements of animal studies would not meet current challenges, as there are too many species differences at the molecular and physiological levels (Perel et al., 2007; Seok et al., 2013). In addition, following extensive testing, evidence has been provided suggesting that human iPSC-derived myocytes may require additional refinement and validation data before they can provide the necessary predictivity and be adopted as a replacement for TQT (Qu, Gao, Fang, & Vargas, 2013; Qu & Vargas, 2015). In particular, these systems have so far proven unable to faithfully replicate the biophysical and pharmacological properties of adult human cardiomyocytes. At the current state of development, even stem cell experts concur that embryonic or iPSC derived myocytes do not exhibit a true adult cardiomyocyte phenotype (Chen, Kim, & Mercola, 2009; Mummery et al., 2003; Scott, Peters, & Dragan, 2013) and do not express all the critical ionic conductances in the quantities and proportions found in adult ventricular cells. Lastly, common conditions with non-genetic causes, such as Type 2 diabetes or ventricular hypertrophy, can result in metabolic and functional changes, which often sensitize the myocardium to drug-induced toxicities. These conditions are difficult, if not impossible, to replicate in immature and generally young myocytes derived from stem cells, but would easily be accessible in a system relying on primary cardiac tissues from organ donors.

Cardiac tissues isolated from the hearts of different animal species have been widely used to conduct cardiac research using a range of biochemical, electrophysiological, pharmacological and morphological approaches, in order to assess the pro-arrhythmic potential of drugs (Akar & Rosenbaum, 2003; Bussek et al., 2012; Rosen, 2001). While access to animal tissues is typically plentiful, the availability of human cardiac samples is limited. When available, human tissues have typically been limited to fixed or frozen samples or very small amounts of fresh and viable tissues which were obtained from surgical discards (Boukens et al., 2015; Brandenburger et al., 2012; Jost et al., 2005, 2013; Näbauer & Kääh, 1998; Näbauer, Beuckelmann, Überfuhr, & Steinbeck, 1996; Wettwer, Amos, Posival, & Ravens, 1994; Wettwer et al., 1993). However, in the past, tissue recovery procedures, as well as tissue quality and quantity have been extremely variable, resulting in an unreliable source for robust and reproducible drug safety data. Consequently, the systematic utilization of human cardiac tissues for detecting drugs that induce arrhythmia has been non-existent.

If properly implemented, the use of human tissue-based assays could provide an important addition to existing methodologies and has a great potential to increase R&D productivity by establishing a novel human-relevant drug safety assessment strategy. The main motivation of this investigation was to develop and validate a human ex-vivo action potential (AP)-based model that uses human ventricular trabeculae, combined with sharp-electrode continuous recordings of the AP to provide a more predictive preclinical approach for assessing pro-arrhythmic risk in man. In particular, we set out in this pilot study to: (i) determine the stability and variability in measurements performed

**Table 1**  
Donor characteristics.

Heart #	Donor identifier	Age	Sex	Ethnicity	BMI	COD	EF (%)
1	140829HHA	47	F	African American	31	CVA/ICH	60
2	140911HHA	47	M	Caucasian	26	Anoxia	70
3	141029HHA	21	M	Caucasian	25	Anoxia	55
4	141208HHA	49	F	Caucasian	34	CVA/ICH	65
5	150215HHA	53	F	African American	27	CVA/ICH	60
6	150227HHA	24	F	Caucasian	35	CVA/ICH	60
7	150323HHA	58	F	Caucasian	27	CVA/ICH	55
8	150409HHA	54	M	Caucasian	21	Anoxia	60
9	150414HHA	37	M	Hispanic	25	CVA/ICH	55
10	150417HHA	52	F	Caucasian	31	HT/ICH	60
11	150424HHA	45	F	African American	31	CNS tumor	65
12	150506HHA	51	M	Caucasian	29	Trauma	71
13	150518HHA	58	F	Caucasian	28	Head trauma	74
14	150522HHA	21	M	Caucasian	23	Head trauma	65
15	150605HHA	56	F	Hispanic	24	CVA/ICH	65
16	150612HHA	40	M	Caucasian	33	Anoxia	65
17	150616HHA	50	M	Hispanic	35	CVA/ICH	70
18	150626HHA	57	F	Caucasian	26	CVA	77
19	150706HHA	19	F	Caucasian	24	Head trauma	70
20	150718HHA	25	M	Hispanic	22	ICH/Stroke	65

F, female; M, male; BMI, body mass index; COD, cause of death, EF, ejection fraction; CVA, cerebrovascular accident; ICH, intracranial haemorrhage; HT, head trauma; CNS, central nervous system; HHA, human heart AnaBios.

from different donor hearts and from different tissue samples from the same heart; (ii) test the effects of 3 torsadogenic (dofetilide, d,l-sotalol, quinidine) and 2 non-torsadogenic (verapamil, paracetamol) drugs in blinded experiments with an emphasis on three recognized pro-arrhythmia predictors (i.e., beat-to-beat variability of AP repolarization, quantified as short-term variability of the AP duration at 90% repolarization (STV(APD90), triangulation (APD90-APD30) and incidence of early afterdepolarizations (EADs); Hondeghem, 2016); and (iii) assess the correlation of these parameters with the incidence of TdP in man.

## 2. Methods

### 2.1. Donor heart procurement

All human tissues used for this study were obtained by legal consent from organ donors in the United States. Donor characteristics and exclusion criteria are shown in Tables 1 and 2, respectively.

**Table 2**  
Donor exclusion criteria.

Age	<14 or >60 year-old
Cardiac disease	Hypokinesia, cardiomyopathy, atrial fibrillation, cardiomegaly, Wolff-Parkinson-White syndrome, endocarditis, left ventricular hypertrophy, coronary artery disease, ischemic heart disease, atherosclerotic heart disease, coronary heart disease
Ejection fraction	<50%
Body mass index	<18 or >35
Infection	HIV, HBV, HCV, MRSA, ongoing infection, positive blood culture
Donor after cardiac death	Anoxia (blood pH at admission <7.0), downtime >20 min, transit time >20 h

**Table 3**

Tissue exclusion criteria.

Resting membrane potential	<−80 mV
APD90 at 1 Hz	<207 ms or >387 ms
Amplitude of the AP	<100 mV
STV at 1 Hz	>2 ms
Tissue response	No AP upon stimulation at baseline
Tissue health	Interruption of perfusion/oxygenation
Drug exposure	Timing of exposure not respected
Positive control	Lack of effect

## 2.2. Tissue preparation, electrophysiological recordings, experimental design and preparation of test articles

Upon arriving at our laboratory, the heart was re-perfused with a cold (approximately 4 °C) proprietary cardioplegic solution. Trabeculae were then dissected from the inner endocardial wall of the ventricle

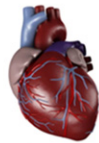
using micro-scissors and tweezers, and transferred to the recording chambers.

Trabeculae were placed in separate, custom-made glass recording chambers (Radnoti LLC) that were perfused with gassed (95% O<sub>2</sub>/5% CO<sub>2</sub>) Tyrode's solution of the following composition (in mM): NaCl 136, KCl 4, MgCl<sub>2</sub> 0.5, NaHCO<sub>3</sub> 12, NaH<sub>2</sub>PO<sub>4</sub> 0.35, Dextrose 11.1, CaCl<sub>2</sub> 1.8, HEPES 10 (pH 7.4). The preparations were fixed at the bottom of the recording chambers and continuously perfused with gassed Tyrode's solution at a rate of 5 ml/min. The temperature in the recording chambers was maintained at approximately 37 °C. Trabeculae were stimulated through a DS8000 digital stimulator (World Precision Instruments) at a pacing rate of 1 Hz with a voltage of 3 V and a pulse width of 3 ms for 30 to 60 min to allow the trabeculae to stabilize. Then, the following stimulation parameters were used: stimulation voltage of 1.5-fold the threshold for AP generation, pulse width 3 ms, pacing rates of 1 and 2 Hz to mimic normal and fast heart rates, respectively. Intracellular potentials were recorded with glass micropipettes filled with 3 M

### Drugs tested in a blinded manner

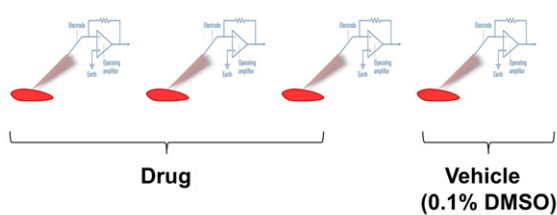


**Dofetilide** (1; 10; 100nM)  
**D,L-Sotalolol** (1; 10; 100μM)  
**Quinidine** (0.1; 1; 10μM)  
**Verapamil** (0.01; 0.1; 1μM)  
**Paracetamol** (2; 20; 200μM)



**5 hearts for each one of the 5 drugs**

### 4 trabeculae from each heart



Perfusion Article	Vehicle	Conc. #1	Conc. #2	Conc. #3
Time (min)	25 3 3	25 3 3	25 3 3	25 3 3
Pacing (Hz)	1 2 1	1 2 1	1 2 1	1 2 1

**Fig. 1.** Experimental protocol. The protocol consisted of measuring APs from individual human ventricular trabeculae over a period of 2 h using sharp-electrode recordings of the membrane potential. Baseline AP stability was assessed by continuous recording for 31 min in control vehicle (Tyrode's, 0.1% DMSO) at pacing rates of 1 Hz (25 min), 2 Hz (3 min) and 1 Hz (3 min). Subsequently, 3 cumulative concentrations of the test article were applied while repeating the same 31-minute pacing protocol for each subsequent drug concentration. For each heart, 3 tissue samples were tested with vehicle control followed by test article and one tissue was used as a vehicle time control. Each one of the 5 drugs was assessed in 5 hearts.

**Table 4**

Distributions of values of the AP parameters in human ventricular trabeculae.

	Variable	Pacing rate	APD30	APD50	APD90	Triangulation	STV
Baseline values (ms)	Mean ± SEM	1 Hz	174 ± 3	234 ± 4	317 ± 5	144 ± 4	0.48 ± 0.03
		2 Hz	122 ± 3*	168 ± 3*	244 ± 4*	121 ± 3*	0.71 ± 0.05*
	Minimum	1 Hz	103	156	224	84	0.07
		2 Hz	65	89	145	70	0.10
	Maximum	1 Hz	302	373	471	309	2.02
		2 Hz	204	255	347	225	3.21
	Median	1 Hz	172	230	311	135	0.42
		2 Hz	118	163	243	115	0.61
	Quartile 1	1 Hz	150	207	282	121	0.29
		2 Hz	108	150	220	103	0.42
	Quartile 3	1 Hz	189	252	344	161	0.64
		2 Hz	137	183	271	135	0.86
Absolute Δ (rate adaptation; ms)	Mean ± SEM		52 ± 2	66 ± 2	74 ± 3	23 ± 2	0.37 ± 0.04
	Minimum		5	27	28	0.35	0.009
	Maximum		98	122	152	122	2.46
	Median		50	63	69	19	0.24
	Quartile 1		40	50	57	12	0.09
	Quartile 3		61	78	85	29	0.49

Absolute Δ, Absolute delta was calculated as the difference between 1 and 2 Hz values of an AP parameter; differences were tested for statistical significance using the paired (two sample for means) Student's *t*-test.

\* *P* < 0.05 versus values at 1 Hz pacing rate.

KCl, with tip resistances between 10 and 20 M $\Omega$ . The micropipette was connected to the headstage of a Neuroprobe amplifier model 1600 (A-M systems Inc.). AP signals were acquired by AP software (LabChart, ADInstruments Inc.) at a sampling rate of 20 kHz. Tissue AP exclusion criteria are shown in Table 3. Although 8 out of the 96 trabeculae investigated in this study had APD90 values above the criterion of 387 ms, these 8 trabeculae exhibited similar drug effects compared to trabeculae with APD90 <387 ms.

Fig. 1 illustrates the experimental protocol used for this study to measure APs. Baseline AP stability was assessed by continuous recording for 31 min in vehicle control (Tyrode solution containing vehicle (0.1% dimethyl sulphoxide, DMSO)) at pacing rates of 1 Hz (25 min), 2 Hz (3 min) and 1 Hz (3 min). Subsequently, 3 cumulative concentrations of the test article were applied while repeating the same 31-min pacing protocol for each drug concentration. For each heart, 3 tissue samples were tested with vehicle control followed by test article and one tissue was tested with vehicle and used as a stability control in the time domain. Each of the drugs was assessed in 5 hearts ( $n = 15$  trabeculae for each drug). The reference drugs selected for this investigation consisted of 3 torsadogenic (dofetilide, d,l-sotalol, quinidine) and 2 non-torsadogenic (verapamil, paracetamol) drugs. The same dilution factor was applied for all drugs in all experiments. Prior to the start of the study, the identity of the drugs was concealed by a third party not involved in any other aspect of the study, in order to allow for the complete blinding of the data collection and analysis.

### 2.3. Data analysis

Following acquisition of the data, offline analysis was carried out using LabChart software and APD was measured at 30, 50 and 90% repolarization (APD30, APD50 and APD90). Data for each experimental condition were expressed as the mean of 30 consecutive APDs at a pacing rate of 1 or 2 Hz. The difference of APD90–APD30 was analyzed to describe AP triangulation. Beat-to-beat variability in repolarization was quantified as STV from APD90 Poincaré plots over a period of 30 s calculated as  $\frac{\sum |APD90_{n+1} - APD90_n|}{(30 \times \sqrt{2})}$ , where APD90 $_n$  and APD90 $_{n+1}$  are the APDs for the  $n$ th AP and the following one, respectively. An EAD was identified as abnormal depolarization during phase 2 or phase 3 of the AP, which was caused by an increase in the frequency of abortive APs before normal repolarization was completed. A decrease in excitability was identified when the stimulus did not initiate an AP during the effective refractory period. The % change for each vehicle control application or reference drug was calculated as the *effect minus baseline/baseline*. Results are expressed as mean  $\pm$  standard error of the mean (SEM).

### 2.4. Statistics

#### 2.4.1. Drug treatment effects

Treatment effects were expressed as the relative percent (%) change compared to the sample's specific baseline control period. To assess effect sizes and 95% confidence intervals for each condition, a single linear mixed effect model was run per descriptor variable and pacing rate. The model included compound and concentration level (low, medium, high) as fixed effects, plus the interaction between the two. The donor identifier (see Table 1) was included as a random intercept, to account for organ specific baseline values. This model allowed assessment of variability between hearts, and the residual variation in fact reflected the intra-heart variability. P-values for all treatment conditions originated from the fixed effect tests, basically probing whether a specific treatment induced a change that was different from zero, and were not corrected for multiple testing.

#### 2.4.2. Signal to noise ratio

Signal to noise ratios were generally determined as ratios between the mean values and the standard deviations (SDs) of a parameter.

Two types of signal to noise indicators were assessed: (i) a stability measure for each single AP recording (mean/SD in a sequence of 31 APs, averaged over all available vehicle measurements) and (ii) a within-tissue stability measure indicating the variability across different recordings of the 31-minute recording cycles (mean/SD in vehicle time controls of a specific tissue sample, averaged over all dedicated control samples).

#### 2.4.3. Activity thresholds

Activity thresholds were defined as the smallest changes that could be reliably detected with the given parameter evaluated. We estimated the distribution of 'blank' measurements by analyzing the random signal changes obtained by the 31-minute cycle-to-cycle switches in the

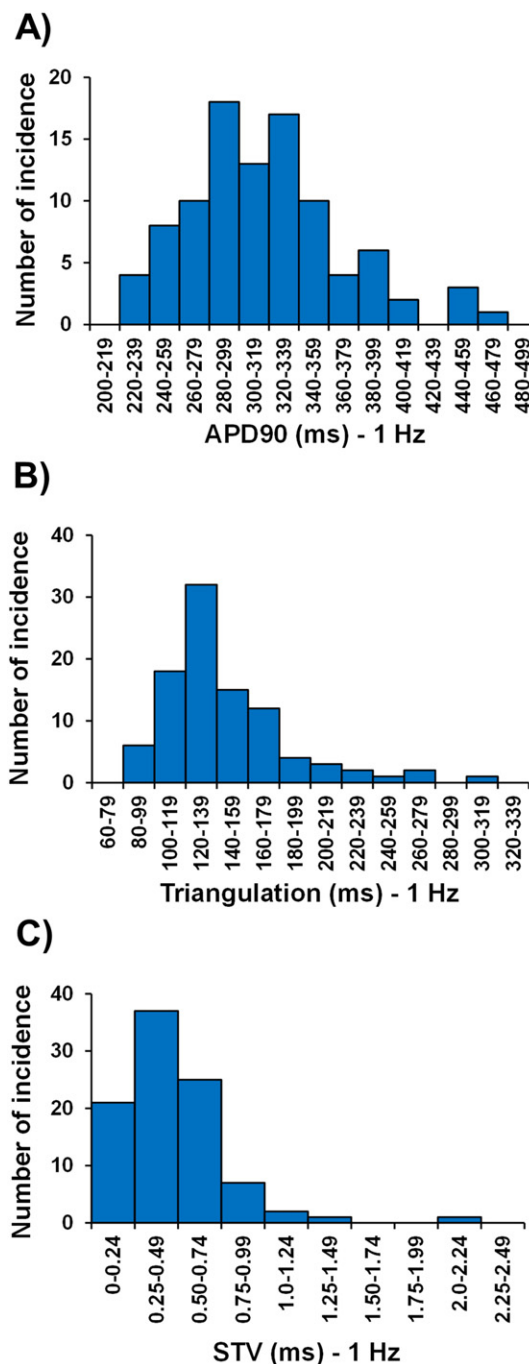


Fig. 2. Distribution histograms of APD90, triangulation and STV in human ventricular trabeculae at a pacing rate of 1 Hz.



dedicated vehicle time controls. Activity thresholds were determined as the 95 percentile of all those random changes, which corresponded to specifying a tolerable false positive rate of 5%. If a change larger than the activity threshold was observed, the presence of a real treatment effect was assumed. This approach was analogous to a frequently used definition of the Limit of Detection. The R quantile function was used to estimate the 95 percentiles. In order to stabilize the results, the highest numerical value from the distribution of blanks was removed if it was regarded as an outlier (Grubb's test P value < 0.01).

#### 2.4.4. Stability in the time domain

Small, but measurable differences existed between the 31-minute cycles recorded for one sample, as could be shown with the 4 consecutive 31-minute vehicle cycles measured for dedicated control tissues. To pick up any non-random drift in time, a linear mixed effect model was used to regress the mean value of each descriptor across one trace against the 31-minute cycle number (1st to 4th cycle). Random intercept and slope were permitted based on the factor of tissue sample. The slope (fixed effect of cycle variable) was taken to reflect the average change of the descriptor from one 31-minute cycle to the next. P values were from the fixed effect test (estimated slope versus the zero slope).

#### 2.4.5. Sample size estimation

Statistical power analysis simulated various scenarios of experiments with a different number of donor hearts and a different number of trabecula samples prepared from those organs. The individual variance components of the heart and trabecula level were estimated using the linear mixed effect model described under in 2.4.1. Based on these SDs, simulations of experimental scenarios were performed with a different number of donor organs and trabeculae per heart (R script). This allowed assessment of the activity thresholds and the statistical power to detect changes of the reference drug treatments, (e.g., the

respective activity threshold or the actually observed changes with the profiled reference drugs) and proposal of reasonable screening strategies.

#### 2.4.6. Assessment of variability

The intra-heart and inter-heart total variabilities were evaluated as follows. For each drug, the mean and SD of the percent change effect in the triplicate trabeculae from each heart were calculated separately for each of the three test concentration periods. For each concentration period, the intra-heart variability was then calculated as the average of the all of the SDs generated from all of the individual hearts for all of the five different drug treatments. Total variability, was calculated as the SD of the mean percent change effect of all of the trabeculae pooled at each concentration period for all reference drugs.

### 3. Results

#### 3.1. Baseline characteristics of the AP in human ventricular trabeculae

A fundamental property of cardiac myocytes is the ability to adapt to an increase in the heart rate with a decrease in APD. Rate-dependent decrease in APD was investigated in the 96 human ventricular trabeculae from the 20 hearts used in this study by measuring APD in the baseline vehicle control period at pacing rates of 1 and 2 Hz. The increase in pacing rate resulted in a decrease in APD30, APD50, APD90 and triangulation, although it increased STV (Table 4). The distributions of the AP parameters from all the vehicle baseline control periods were further analyzed and compared for APD30, APD50, APD90, triangulation and STV at 1 and 2 Hz pacing rates (Fig. 2; Supplementary Figs. 1 and 2; Table 4).

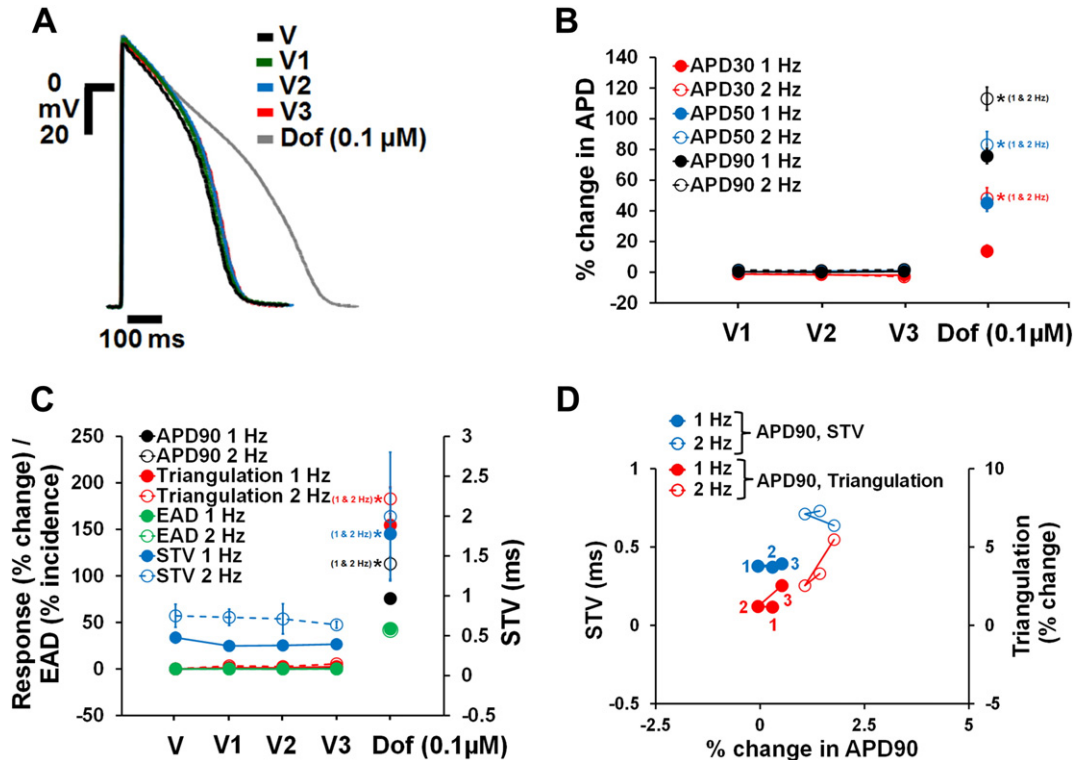


**Fig. 3.** Stability of AP recordings over time in human ventricular trabeculae. (A) Typical APs recorded from a human ventricular trabecula at a pacing rate of 1 Hz in the presence of vehicle control and after exposure to 0.1 μM dofetilide, the positive control. V1, V2 and V3 correspond to the 1st, 2nd and 3rd applications of vehicle (n = 21). (B) Mean % changes in APD30, APD50 and APD90 induced by 3 sequential additions of vehicle and after exposure to dofetilide at 1 and 2 Hz. (C) Mean changes in APD90, triangulation, STV and EAD incidence when trabeculae were incubated with vehicle and dofetilide at 1 and 2 Hz. Note that the effects of vehicle and dofetilide on APD90/triangulation/EAD activity and STV are plotted on a separate y-axis. (D) Effects of 3 sequential additions of vehicle on STV and triangulation as a function of change in APD90 in human ventricular trabeculae at pacing rates of 1 and 2 Hz. Note that the effects of vehicle on STV and triangulation are plotted on a separate y-axis. 1/1, 2/2 and 3/3 correspond to V1, V2 and V3 of vehicle, respectively. \*P < 0.05 versus values from vehicle.

### 3.2. Time-control data for AP parameters in human ventricular trabeculae

In order to determine the stability of the human trabecular assay system, we established vehicle time-control data in 21 trabeculae from 20 hearts using 3 additions of vehicle solution to mimic experimental conditions with the active drugs. At a pacing frequency of either 1 or 2 Hz, neither the 1st, 2nd or 3rd vehicle addition significantly affected APD30, APD50 and APD90 in human ventricular trabeculae relative to baseline values of vehicle solution (Fig. 3A and B). The same was true for STV and triangulation (Fig. 3C and D). For example, for the 1 Hz pacing rate, the systematic time related drift in APD90, triangulation and STV were estimated as 0.8, 1.6 and  $-0.04$  ms, respectively,

when changing from one application of vehicle to the next. None of these drifts was statistically significant. Additionally, no incidence of EAD (Fig. 3C) or decrease in excitability was observed in the presence of vehicle control.

Furthermore, all the vehicle control trabeculae responded positively to the positive control ( $0.1 \mu\text{M}$  dofetilide) reinforcing the determined stability and responsiveness of the human tissues. We observed a significant increase in APD, triangulation and STV (Fig. 3A–C), as well as elicited EADs in 9 out of the 21 trabeculae at 1 and 2 Hz pacing rates (Fig. 3C). Additionally,  $0.1 \mu\text{M}$  dofetilide induced decrease in excitability in 14% and 57% of trabeculae stimulated at 1 and 2 Hz, respectively.

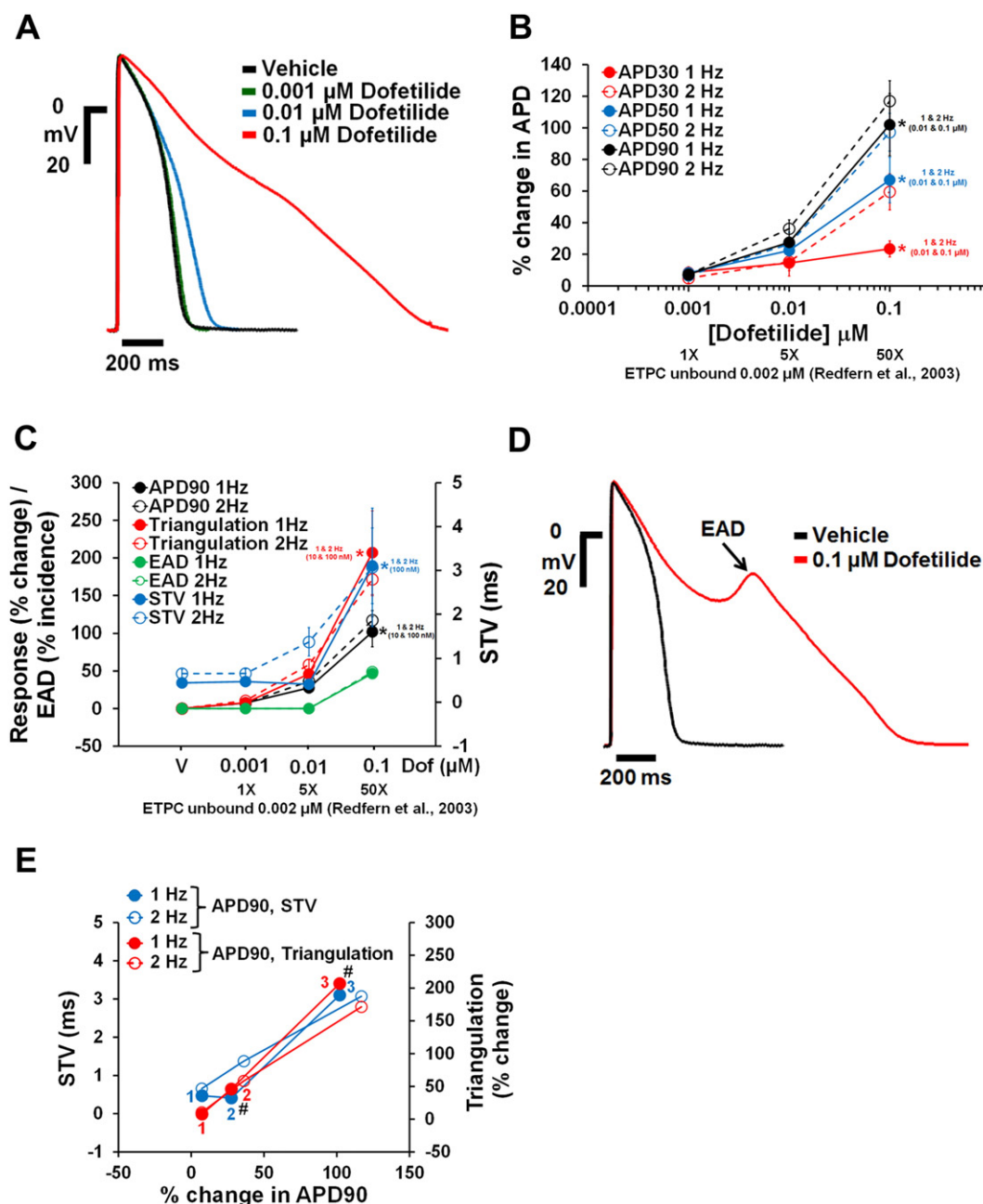


**Fig. 4.** Effects of dofetilide on AP in human ventricular trabeculae. (A) Typical APs recorded from a human ventricular trabecula at a pacing rate of 1 Hz in the presence of vehicle control and after exposure to dofetilide at 0.001, 0.01 and  $0.1 \mu\text{M}$ . (B) Mean % changes in APD30, APD50 and APD90 induced by addition of dofetilide at 1 and 2 Hz ( $n = 15$ ). (C) Mean changes in APD90, triangulation, STV and EAD incidence when trabeculae were incubated with dofetilide at 1 and 2 Hz. Note that the effects of dofetilide on APD90/triangulation/EAD activity and STV are plotted on a separate y-axis. (D) Shows a representative EAD recorded from the same trabecula as in (A) in the presence of  $0.1 \mu\text{M}$  dofetilide and stimulated at 1 Hz. (E) Effects of dofetilide addition on STV and triangulation as a function of change in APD90 in human ventricular trabeculae at pacing rates of 1 and 2 Hz. Note that the effects of dofetilide on STV and triangulation are plotted on a separate y-axis. 1/1, 2/2 and 3/3 correspond to 0.001, 0.01 and  $0.1 \mu\text{M}$  of dofetilide, respectively. #Decrease in excitability was observed after exposure to 0.01 and  $0.1 \mu\text{M}$  dofetilide at 1 and 2 Hz. ETPC, Effective therapeutic plasma concentration. \* $P < 0.05$  versus values from vehicle.

Parameters can be ranked by average signal to noise ratio across samples. Most variables showed a very favorable signal to noise ratio, thus can be reliably measured. The vehicle time controls were also used to determine signal-to-noise ratio for each single AP recording or within trabecula. The data indicated that parameters could be ranked by average signal-to-noise ratio across samples and most variables showed a very favorable ratio. Thus, the favorable signal-to-noise ratio indicated that AP parameters could be reliably measured in the human ex-vivo AP-based model at 1 Hz and 2 Hz. Furthermore, threshold activity flags were calculated as the 95th percentile of all random signal changes observed for vehicle time controls. This implied accepting a 5% false positive rate when setting a threshold at this level and declaring that parameter changes larger than threshold resulted from drug treatment effects. Threshold values for changes over baseline control for APD90, triangulation and STV were found to be 7%, 9% and 102% at 1 Hz pacing frequency, respectively. Similar flags were established at 2 Hz (data not shown).

### 3.3. Effects of reference drugs on APD in human ventricular trabeculae

Dofetilide, d,l-sotalol and quinidine, paracetamol and verapamil are frequently used as reference drugs, which are expected to either increase (the first 3) or have no effects (the latter 2) on APD, respectively. APD responses to these reference drugs in human ventricular trabeculae are shown in Figs. 4–8. Dofetilide (Fig. 4A–B), d,l-sotalol (Fig. 5A–B) and quinidine (Fig. 6A–B) caused concentration-dependent prolongations of the APD90. While dofetilide and d,l-sotalol exhibited significant increases in APD30, APD50 and APD90 at 5-fold and 0.7-fold their unbound effective therapeutic plasma concentrations (ETPC),

respectively, quinidine only increased APD90, but had no effect on APD30 or APD50 at concentrations up to 3-fold the unbound ETPC. While paracetamol caused no changes in APD30, APD50 and APD90 up to 14.7-fold its free ETPC (Fig. 7A–B), verapamil decreased APD30 at 12.4-fold its free ETPC with no effect on APD50 or APD90 (Fig. 8A–B). The effect of the positive control (0.1  $\mu$ M dofetilide) was observed in all trabeculae tested with paracetamol and verapamil (Figs. 7A–B and 8A–B).

### 3.4. Effects of reference drugs on pro-arrhythmia markers in human ventricular trabeculae

We sought to determine which pro-arrhythmia markers derived from the human ventricular trabeculae studies could be used to differentiate torsadogenic from non-torsadogenic drugs. In addition to the changes in APD, data showed concentration dependent increases in triangulation and STV in human ventricular trabeculae, with dofetilide, d,l-sotalol and quinidine. Dofetilide demonstrated increases in both triangulation and STV at both 1 and 2 Hz pacing rates (Fig. 4C and E). In contrast to the STV increases at 50-fold the free ETPC, the increase in triangulation became statistically significant already at 5-fold the free ETPC (Fig. 4C). dofetilide elicited EADs only at 0.1  $\mu$ M in 7 out of 15 trabeculae at both 1 and 2 Hz (Fig. 4C and D). Additionally, 0.01  $\mu$ M dofetilide caused decrease in excitability in 2 out of 15 trabeculae at 2 Hz while 0.1  $\mu$ M dofetilide caused decrease in excitability in 1 out of 15 trabeculae at 1 and 2 Hz after exposure, respectively (Fig. 4E).

Similarly to dofetilide, d,l-sotalol increased STV in a concentration-dependent manner at 1 and 2 Hz pacing rates (Fig. 5C and D), and the

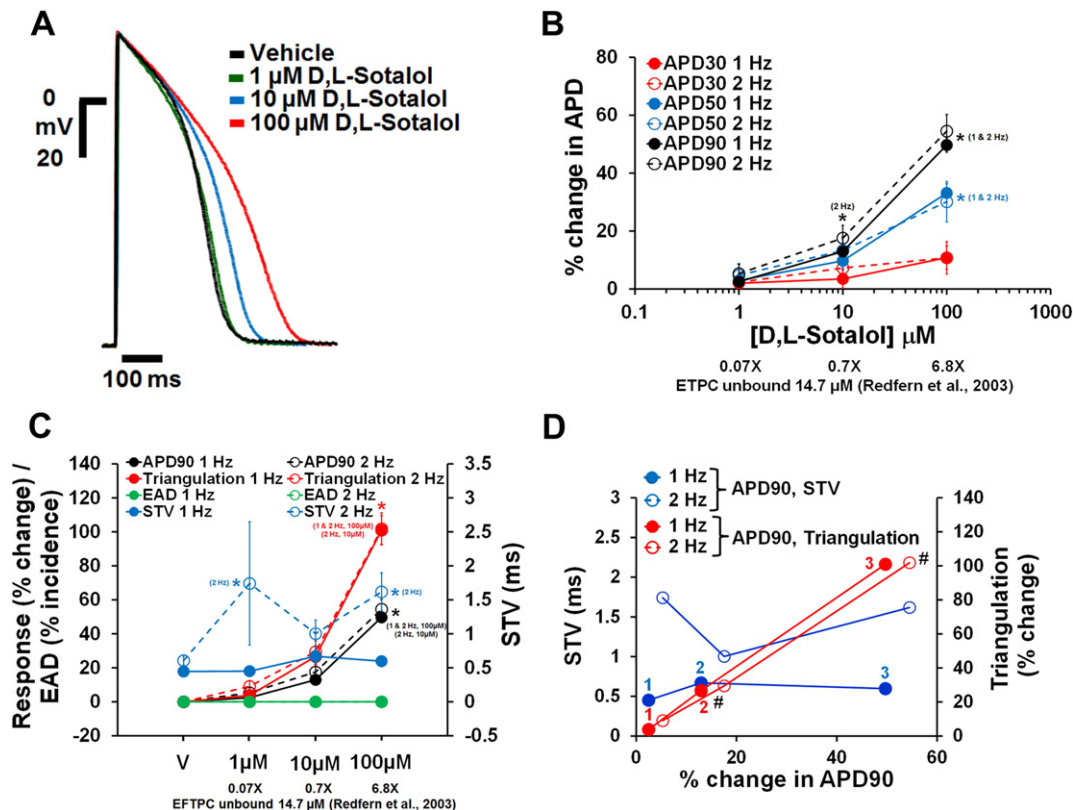


**Fig. 5.** Effects of d,l-sotalol on AP in human ventricular trabeculae. (A) Typical APs recorded from a human ventricular trabecula at a pacing rate of 1 Hz in the presence of vehicle control and after exposure to d,l-sotalol at 1, 10 and 100  $\mu$ M. (B) Mean % changes in APD30, APD50 and APD90 induced by addition of d,l-sotalol at 1 and 2 Hz (n = 15). (C) Mean changes in APD90, triangulation, STV and EAD incidence when trabeculae were incubated with d,l-sotalol at 1 and 2 Hz. Note that the effects of d,l-sotalol on APD90/triangulation/EAD activity and STV are plotted on a separate y-axis. (D) Effects of d,l-sotalol addition on STV and triangulation as a function of change in APD90 in human ventricular trabeculae at pacing rates of 1 and 2 Hz. Note that the effects of d,l-sotalol on STV and triangulation are plotted on a separate y-axis. 1/1, 2/2 and 3/3 correspond to 1, 10 and 100  $\mu$ M of d,l-sotalol, respectively. #Decrease in excitability was observed after exposure to 10 and 100  $\mu$ M d,l-sotalol at 2 Hz. ETPC, Effective therapeutic plasma concentration. \*P < 0.05 versus values from vehicle.

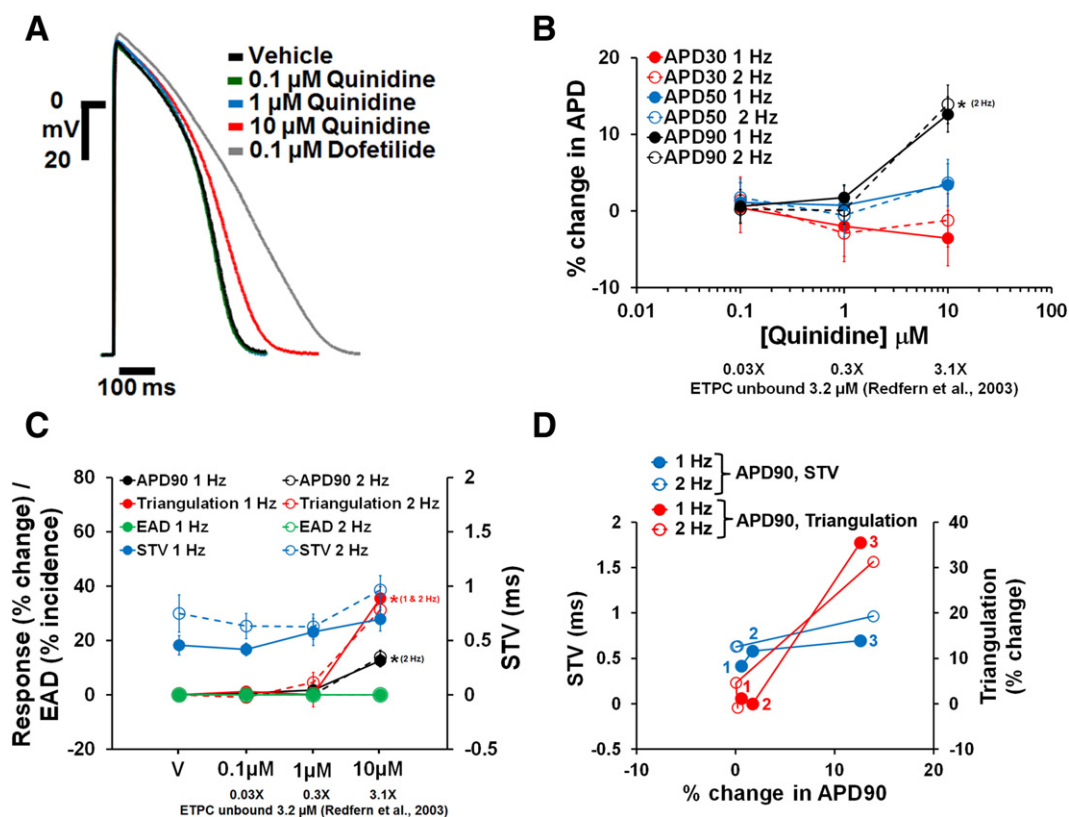


**Fig. 6.** Effects of quinidine on AP in human ventricular trabeculae. (A) Typical APs recorded from a human ventricular trabecula at a pacing rate of 1 Hz in the presence of vehicle control and after exposure to quinidine at 0.1, 1 and 10 μM. (B) Mean % changes in APD30, APD50 and APD90 induced by addition of quinidine at 1 and 2 Hz ( $n = 15$ ). (C) Mean changes in APD90, triangulation, STV and EAD incidence when trabeculae were incubated with quinidine at 1 and 2 Hz. Note that the effects of quinidine on APD90/triangulation/EAD activity and STV are plotted on a separate y-axis. (D) Effects of quinidine addition on STV and triangulation as a function of change in APD90 in human ventricular trabeculae at pacing rates of 1 and 2 Hz. Note that the effects of quinidine on STV and triangulation are plotted on a separate y-axis. 1/1, 2/2 and 3/3 correspond to 0.1, 1 and 10 μM of quinidine, respectively. ETPC, Effective therapeutic plasma concentration. \*\* $P < 0.05$  versus values from vehicle.

increase in STV at 2 Hz became statistically significant at 0.07-fold the ETPC. Moreover, d,l-sotalol data showed a significant increase in triangulation with increasing concentrations of 1 and 2 Hz (Fig. 5C and D). The increase in triangulation also became statistically significant at the free ETPC (Fig. 5C). Even though STV and triangulation increased significantly, d,l-sotalol elicited no EADs at 1 or 2 Hz (Fig. 4C). However, decrease in excitability was observed at 2 Hz in 1 out of 15 trabeculae and 2 out of 15 trabeculae after exposure to 10 and 100 μM, respectively. Finally, quinidine increased STV and triangulation after exposure to the highest test concentration at 1 and 2 Hz (i.e., 3-fold the ETPC; Fig. 6C and D). None of the trabeculae demonstrated EAD events and decrease in excitability in presence of quinidine up to 3-fold the ETPC (Fig. 6C and D).

Neither paracetamol (Fig. 7C and D) nor verapamil (Fig. 8C and D) at increasing concentrations showed effects on STV and triangulation at pacing rates of 1 or 2 Hz. However, addition of the positive control (0.1 μM dofetilide) to the trabeculae tested with both paracetamol and verapamil increased STV and triangulation, and induced EADs (Figs. 7C and 8C). Furthermore, the incidence of dofetilide-induced decrease in excitability was seen in trabeculae tested with paracetamol (7% and 64% at 1 and 2 Hz, respectively) and verapamil (47% at 2 Hz only). Finally, multi-parametric analysis of the AP variables including APD90, Triangulation and STV at 1 and 2 Hz demonstrated that the assessment of these variables could provide a model for the differentiation of torsadogenic from non-torsadogenic reference drugs and for a determination of their pro-arrhythmic risk with respect to the therapeutic index (Figs. 4E, 5–8D; Supplementary Fig. 3).

### 3.5. Variability in AP measurements from human ventricular trabeculae and estimation of sample size

In order to determine the reproducibility and reliability of the human trabeculae assay system, we further assessed the intra-heart and inter-heart (Total) variability of tissue responses. Total variability for AP parameters in the presence of vehicle controls at 1 and 2 Hz is shown in Fig. 9 and Supplementary Fig. 4, respectively. For example, the highest total SDs related to the mean percent change in APD90 were 4.2 and 5.7 at 1 and 2 Hz pacing rates, respectively (Fig. 9A). Additionally, our data showed that the intra-heart variability for APD90, triangulation and STV accounted for almost 80–90% of the Total observed variability for each of these AP parameters after exposure to drug concentration at 1 (Fig. 9) and 2 Hz (Supplementary Fig. 4). For the inter-heart variability for the drug concentration period corresponding to 10-fold the ETPC, the total SD related to the mean percent change in APD90 effects at a pacing rate of 1 Hz was 8.7, while the intra-heart SD for the same period was 7.8 (Fig. 9A). Similar APD90 variability was observed at 2 Hz (Supplementary Fig. 4A). Taken together, these data establish that the inter-donor variability is relatively small and does not add significant noise beyond what is inherent to this experimental approach.

The observed variability was also included in the estimation of sample size (Fig. 10; Supplementary Fig. 5). Based on the analysis of variability and by applying statistical power analyses, our data indicate that a sample size of at least 2 donor hearts and 3 human ventricular trabeculae per heart would be sufficient to detect drug-induced AP effects for



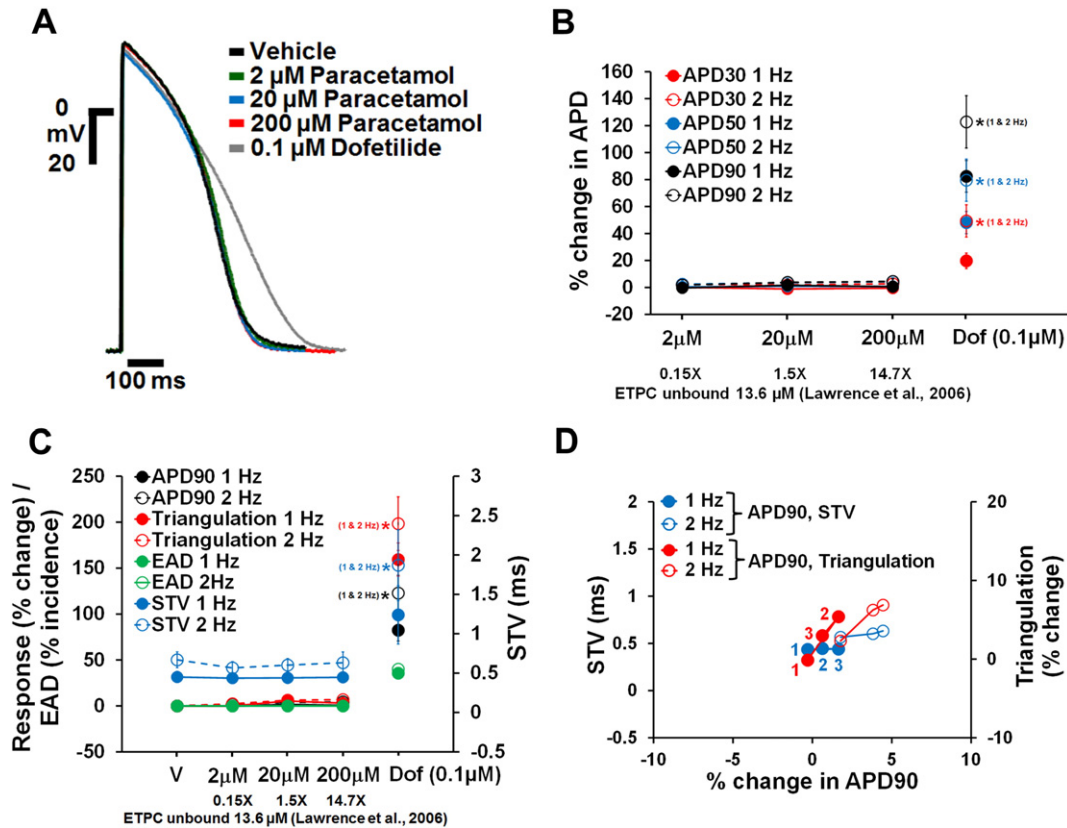


**Fig. 7.** Effects of paracetamol on AP in human ventricular trabeculae. (A) Typical APs recorded from a human ventricular trabecula at a pacing rate of 1 Hz in the presence of vehicle control, and after exposure to paracetamol (2, 20 and 200 μM) and 0.1 μM dofetilide (the positive control). (B) Mean % changes in APD30, APD50 and APD90 induced by addition of paracetamol and after exposure to dofetilide at 1 and 2 Hz ( $n = 15$ ). (C) Mean changes in APD90, triangulation, STV and EAD incidence when trabeculae were incubated with paracetamol and dofetilide at 1 and 2 Hz. Note that the effects of paracetamol and dofetilide on APD90/triangulation/EAD activity and STV are plotted on a separate y-axis. (D) Effects of paracetamol addition on STV and triangulation as a function of change in APD90 in human ventricular trabeculae at pacing rates of 1 and 2 Hz. Note that the effects of paracetamol on STV and triangulation are plotted on a separate y-axis. 1/1, 2/2 and 3/3 correspond to 2, 20 and 200 μM of paracetamol, respectively. ETPC, Effective therapeutic plasma concentration. \*\*\* $P < 0.05$  versus values from vehicle.

the concentration of around 10-fold the ETPC of dofetilide (0.01 μM), d,l-sotalol (100 μM) or quinidine (10 μM) (target power 80%).

#### 4. Discussion

The main findings of the present study can be summarized as follows: (i) the human ex-vivo AP-based model was found to be electrophysiologically stable; (ii) the model provided quantitative activity flags; (iii) the relatively low total variability of the pharmacological responses in the tissues allowed for a favorable signal to noise ratio and the identification of pro-arrhythmic signal; (iv) a sample size of at least 2 hearts and 3 trabeculae per heart would be required to detect drug-induced AP effects; (v) the experimental system provided the possibility to clearly differentiate between pro-arrhythmic and non-pro-arrhythmic drugs by measuring several AP-related parameters; and (vi) our findings support the potential of this human-based model to significantly enhance preclinical cardiac risk assessment.

The availability of quality viable human adult heart tissue for cardiac safety studies has been a challenge (Holmes et al., 2015). In a focused effort to overcome these limitations, we have set out to first optimize tissue procurement logistics, tissue harvesting and handling methods, and standardized recovery and shipping methods across numerous tissue procurement facilities. These efforts helped establish our capability to procure high quality viable human heart samples on a scale that is unprecedented. A great part of our efforts has been spent on the development of proprietary perfusion and reperfusion solutions and methodologies, which consistently allow for the preservation of cardiac tissue viability and functionality. Moreover, our human ex-vivo AP-based model is electrophysiologically stable, displays the fundamental

property of reverse-rate dependence (see O'Hara, Virág, Varró, & Rudy, 2011), demonstrates relative homogenous electrophysiological characteristics (Fig. 2; Supplementary Figs. 1 and 2) and provides stable AP recordings for experiments of over 2 hour duration (Fig. 3). Moreover, the absence of systematic trends over time confirmed that the health and functionality of trabeculae were preserved. Additionally, favorable signal to noise ratio and activity flags indicated that AP parameters can be reliably measured in our human ex-vivo AP-based model. Additionally, our data indicate that 2 hearts and 3 trabeculae per heart would be required to detect dofetilide- and d,l-sotalol-induced effects on APD90 and triangulation at a concentration of around 10-fold the ETPC (Fig. 10). While the detection of quinidine effects requires the same number of hearts, 3 and 4 trabeculae would be necessary to identify quinidine effects on triangulation and APD90, respectively. Testing of quinidine at only 3-fold its ETPC could be an important contributing factor to the difference observed in the estimation of trabecula size. Since novel drugs will be tested at multiples above their ETPCs, we believe it is therefore appropriate to propose that a sample size of at least 2 hearts and 3 trabeculae per heart would be sufficient to detect drug-induced AP effects in our human ex-vivo AP-based model with 80% power. Despite the small sample size, we conclude that the ex-vivo human based ventricular trabeculae model provides a suitable system to evaluate the acute pro-arrhythmic potential of evolving drugs.

Various academic groups have used, to a very limited extent, cardiac tissues from healthy donors (Boukens et al., 2015; Jost et al., 2005, 2013) and patients (Brandenburger et al., 2012; Nawrath & Eckel, 1979; Näbauer & Käb, 1998; Näbauer et al., 1996; Sivagangabalan et al., 2014; Wettwer et al., 1993, 1994) to investigate the role of ion channels, specifically potassium channels, in human ventricular repolarization.

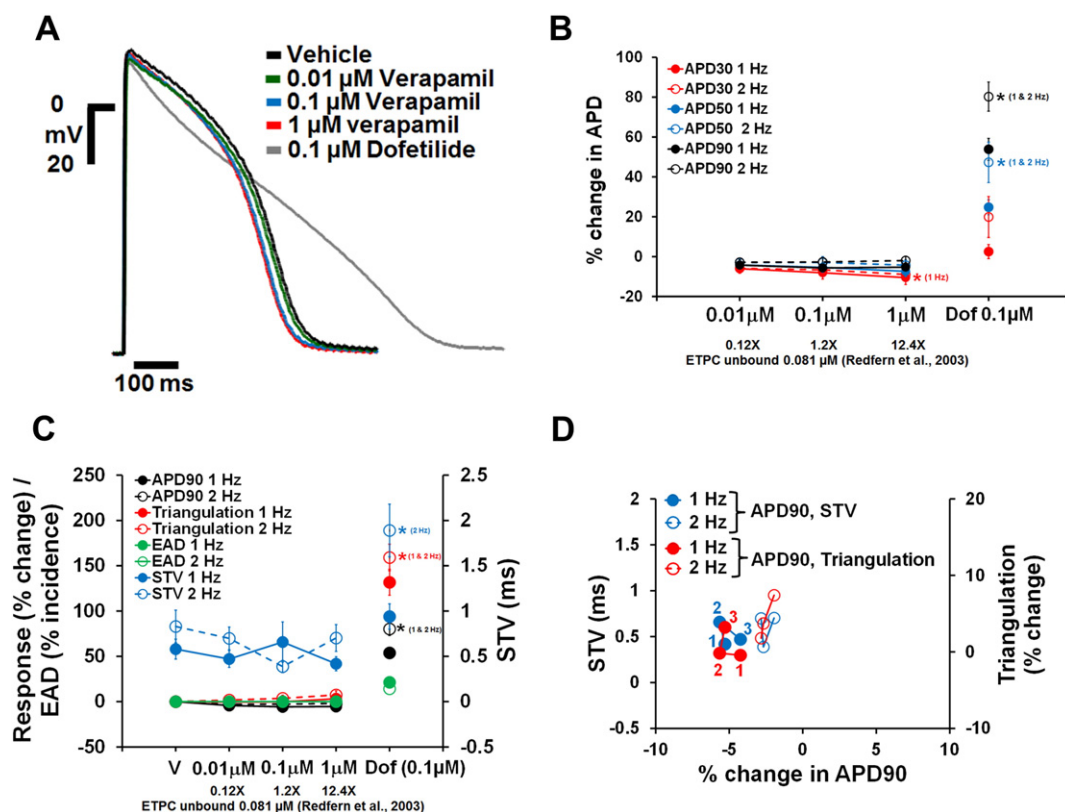


**Fig. 8.** Effects of verapamil on AP in human ventricular trabeculae. (A) Typical APs recorded from a human ventricular trabecula at a pacing rate of 1 Hz in the presence of vehicle control, and after exposure to verapamil (0.01, 0.1 and 1  $\mu$ M) and 0.1  $\mu$ M dofetilide (the positive control). (B) Mean % changes in APD30, APD50 and APD90 induced by addition of verapamil at 1 and 2 Hz ( $n = 15$ ). (C) Mean changes in APD90, triangulation, STV and EAD incidence when trabeculae were incubated with verapamil at 1 and 2 Hz. Note that the effects of verapamil on APD90/triangulation/EAD activity and STV are plotted on a separate y-axis. (D) Effects of verapamil addition on STV and triangulation as a function of change in APD90 in human ventricular trabeculae at pacing rates of 1 and 2 Hz. Note that the effects of verapamil on STV and triangulation are plotted on a separate y-axis. 1/1, 2/2 and 3/3 correspond to 0.01, 0.1 and 1  $\mu$ M of verapamil, respectively. ETPC, Effective therapeutic plasma concentration. \* $P < 0.05$  versus values from vehicle.

Additionally, dofetilide, Sotalol and quinidine have been found to prolong ventricular repolarization in healthy human hearts (QT duration; Johannesen et al., 2014; Lande et al., 1998; Vicente et al., 2015) and patients (QT duration (Echt et al., 1982; McComb, McGovern, McGowan, Ruskin, & Garan, 1987); monophasic AP recordings (Melichercik et al., 1999; Nademanee et al., 1990; Yuan, Wohlfart, Rasmussen, Olsson, & Blomström-Lundqvist, 1994)). Our AP data from healthy donor hearts are in agreement with those reported for dofetilide, Sotalol and quinidine by these groups. Specifically, our data showed that these 3 QT-prolonging drugs increased APD in the human ex-vivo AP-based model and this prolonging effect was seen at concentrations of 1 to 3-fold the unbound ETPCs (Figs. 4–6). Additionally, a uniform prolongation of the AP was observed with d,l-sotalol and quinidine over pacing rates of 1 and 2 Hz (Figs. 5B and 6B). These findings with d,l-sotalol and quinidine are in agreement with those reported on the human monophasic AP by Melichercik et al. (1999) and Nademanee et al. (1990). Similarly, Sager et al. (1993) reported that Amiodarone did not exert rate-dependent effects on human monophasic AP. Moreover, dofetilide exerted rate-dependent effects on APD30 and APD50, but not APD90 (Fig. 4B). In agreement with our data, Yuan et al. reported that the effect of dofetilide on in situ human monophasic APD90 is not rate-dependent (Yuan et al., 1994). In contrast, other studies reported that drug-induced prolongation of ventricular repolarization with dofetilide, sotalol and moxifloxacin was more pronounced with slow pacing rates (Extramiana et al., 2006; Funck-Brentano et al., 1991; Lande et al., 1998; Okada, Ogawa, Sadanaga, & Mitamura, 1996). Therefore, drug action as a function of pacing rate in the human heart warrants further assessment.

Dofetilide, d,l-sotalol and quinidine have been associated with pro-arrhythmic risk (Frommeyer & Eckardt, 2016; Gintant et al., 2016;

Redfern et al., 2003). Human trabeculae yielded information about the ability of dofetilide (Fig. 4C & D), d,l-sotalol (Fig. 5C & D) and quinidine (Fig. 6C & D) to induce measurable changes in pro-arrhythmia markers (APD90, triangulation and STV). Furthermore, dofetilide (Fig. 4D) and d,l-sotalol (Fig. 5D), but not quinidine (Fig. 6D), were found to induce decrease in excitability. We also observed that 0.1  $\mu$ M dofetilide induced EADs in approximately 42% and 50% of the recordings made in vehicle time controls (Fig. 3C) and dofetilide experiments (Fig. 4C & D), respectively. However, no EAD was observed after exposure of trabeculae to the highest concentrations of d,l-sotalol or quinidine. Guo et al. (2011) showed that 0.1  $\mu$ M dofetilide induced EADs in non-failing human myocytes at a pacing rate of 0.25 Hz (see also O'Hara et al., 2011). Also EADs were observed in ventricular trabeculae isolated from failing human hearts after being exposed to modified Tyrode solution containing low levels of potassium and magnesium, and noradrenaline (Vermeulen et al., 1994). In addition, trabeculae are structures with electrically well-coupled cells. Altogether, these data suggest that drug exposure above a certain level of the free ETPC (our study proposes 30 to 50-fold) or modified experimental conditions (other studies) could help creating conditions more favorable to the occurrence of EADs. Our data also illustrate the potential of multi-parametric analysis to differentiate torsadogenic from non-torsadogenic drugs when the effects on STV and triangulation were assessed as a function of change in APD90 (Figs. 4E and 5–8D; Supplementary Fig. 3). Apart from STV triangulation and EAD incidence, other recognized pro-arrhythmia predictors (i.e., spatial dispersion of repolarization; Frommeyer & Eckardt, 2016) could not be assessed in our human ex-vivo AP-based model due to the geometry and size of trabeculae.

We next assessed the effects of verapamil and paracetamol, which were found to have no effects on human ventricular repolarization,

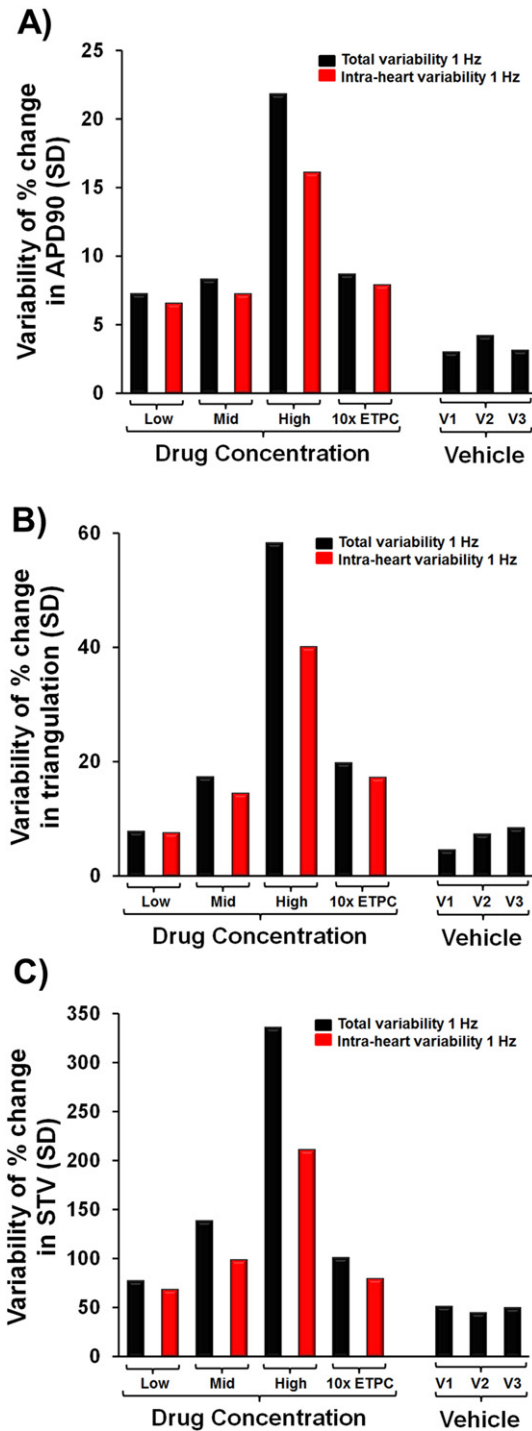


**Fig. 9.** Variability in measurements performed from different donor hearts and from different trabeculae from the same heart. (A), (B) and (C) show the “Total” and “intra-heart” variabilities for APD90, triangulation and STV at a pacing rate of 1 Hz, respectively ( $n = 96$ ). V1, V2 and V3 correspond to the 1st, 2nd and 3rd applications of vehicle. Conc., concentration; SD, Standard deviation; 10× ETPC, 10-fold effective therapeutic plasma concentration.

consistent with the known lack of pro-arrhythmic risk posed by these drugs (Gintant et al., 2016; Lawrence, Bridgland-Taylor, Pollard, Hammond, & Valentin, 2006; Redfern et al., 2003). Our APD data from healthy donor hearts showed that while paracetamol caused no change in APD (Fig. 7A & B), verapamil decreased APD30 with no effect on APD50 and APD90 (Fig. 8A & B). verapamil's lack of effect on late repolarization is in agreement with QT data reported in healthy subjects (Johannesen et al., 2014; Vicente et al., 2015). Additionally, neither

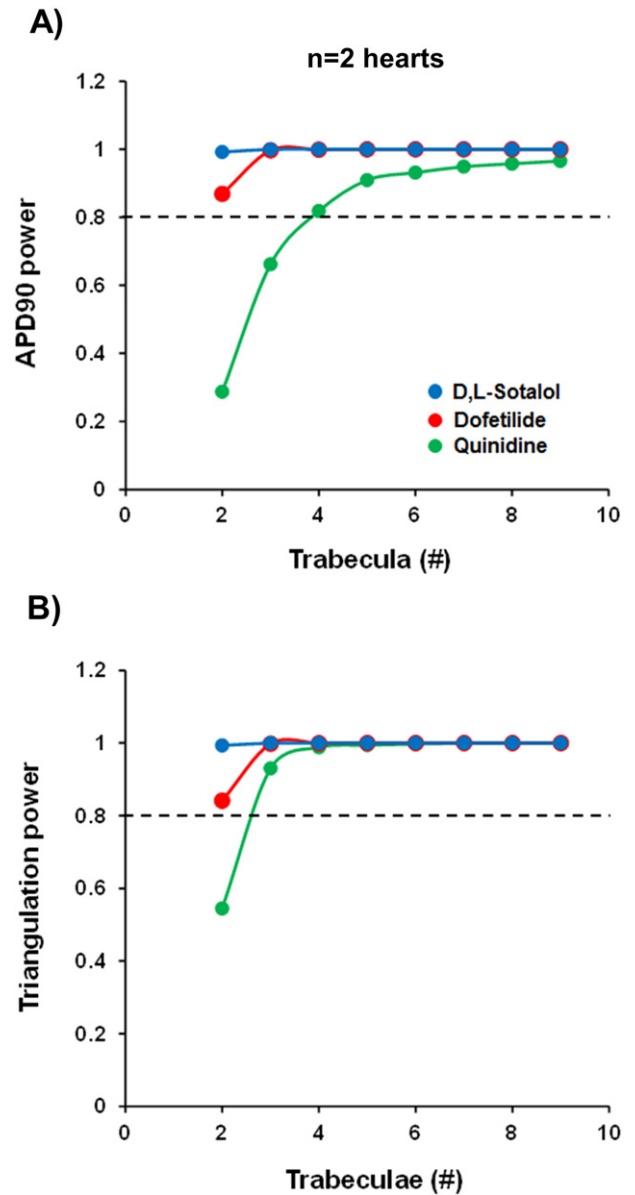


**Fig. 10.** Estimation of sample size with 2 hearts. (A) and (B) show the estimation of sample size for APD90 and triangulation at a pacing rate of 1 Hz for the concentration of around 10-fold the ETPC of dofetilide (0.01  $\mu$ M), d,l-sotalolol (100  $\mu$ M) or quinidine (10  $\mu$ M). Power calculation was performed on a % change scale. Each tissue sample served as its own control. Treatment effect unequal to zero was detected with linear mixed effect model. Target power 80% (dashed black line) corresponds to an 80% chance of concluding there was a real effect.

paracetamol nor verapamil had any effects on pro-arrhythmia markers and no incidence of EAD or decrease in excitability was observed in all trabeculae tested with these two drugs (Figs. 7C & D and 8C & D). While quinidine, which blocks hERG, calcium and late sodium currents, and verapamil, which blocks hERG and calcium currents, are multichannel blockers, only quinidine was found to be associated with pro-arrhythmic risk. This is likely due to quinidine's more pronounced hERG block than calcium and late sodium block (Vicente et al., 2015). Thus, our data suggest that the human ex-vivo AP-based model can potentially differentiate drugs with high versus low pro-arrhythmic risk based on the integrated electrophysiological effects (see also Vicente et al., 2015) providing more holistic insights into drug responses. The ability of APD90, triangulation and STV to respond differentially to perturbations introduced by pro-arrhythmic versus non-pro-arrhythmic drugs constituted a major critical finding of our investigation, although the



confidence in the ability of our human ex-vivo AP-based model to identify drugs with pro-arrhythmic potential can be gradually grown by further evaluating drugs recently selected by the CiPA initiative (Fermini et al., 2016). In addition, the data we have generated with regard to the donor-to-donor variability indicate that the human heart-based approach can be implemented using a feasible number of donor samples, providing both a practical solution and affordable costs. This finding suggests that our experimental system can also be potentially used to evaluate drug safety in the context of comorbidities, poly-pharmacy and aging, by leveraging the epidemiological diversity of the donor population and conducting drug safety studies in non-healthy hearts.

In conclusion, our study addresses a pressing need in the pharmaceutical industry aimed at establishing a novel human pro-arrhythmia assessment strategy. Our human ex-vivo AP-based model would therefore enable drug discovery projects to generate, for the first time, reliable and predictive human-based pro-arrhythmia data at the preclinical stage of drug development. As a consequence, novel drugs to be introduced in clinical studies will have real knowledge of potential cardiotoxicity in humans, resulting in higher success rates for development programs and consequently bringing hope and relief to patients.

Supplementary data to this article can be found online at <http://dx.doi.org/10.1016/j.vascn.2016.05.016>.

## Acknowledgements

This work was supported by a NIH Small Business Innovation Research (SBIR) grant (IR43TR001133-01).

## References

- Akar, F. G., & Rosenbaum, D. S. (2003). Transmural electrophysiological heterogeneities underlying arrhythmogenesis in heart failure. *Circulation Research*, 93, 638–645.
- Anon. (2005a). ICH S7B note for guidance on the nonclinical evaluation of the potential for delayed ventricular repolarization (QT interval prolongation) by human pharmaceuticals. London, 25 May. Reference CHMP/ICH/423/02.
- Anon. (2005b). ICH E14 note for guidance on the clinical evaluation of QT/QTc interval prolongation and proarrhythmic potential for nonantiarrhythmic drugs. London, 25 May. Reference CHMP/ICH/2/04.
- Boukens, B. J., Sulkun, M. S., Gloschat, C. R., Ng, F. S., Vigmond, E. J., & Efimov, I. R. (2015). Transmural APD gradient synchronizes repolarization in the human left ventricular wall. *Cardiovascular Research*, 108(1), 188–196.
- Brandenburger, M., Wenzel, J., Bogdan, R., Richardt, D., Nguemo, F., Reppel, M., et al. (2012). Organotypic slice culture from human adult ventricular myocardium. *Cardiovascular Research*, 93, 50–59.
- Bussek, A., Schmidt, M., Bauriedl, J., Ravens, U., Wettwer, E., & Lohmann, H. (2012). Cardiac tissue slices with prolonged survival for in vitro drug safety screening. *Journal of Pharmacological and Toxicological Methods*, 66(2), 145–151.
- Chen, H. S. V., Kim, C., & Mercola, M. (2009). Electrophysiological challenges of cell-based myocardial repair. *Circulation*, 120, 2496–2508.
- Cook, D., Brown, D., Alexander, R., March, R., Morgan, P., Satterthwaite, G., et al. (2014). Lessons learned from the fate of AstraZeneca's drug pipeline: A five-dimensional framework. *Nature Reviews Drug Discovery*, 13(6), 419–431.
- Echt, D. D., Berte, L. E., Clusin, W. T., Samuelsson, R. G., Harrison, D. C., & Mason, J. W. (1982). Prolongation of the human cardiac monophasic action potential by sotalol. *American Journal of Cardiology*, 50(5), 1082–1086.
- Ewart, L., Aylott, M., Deurincq, M., Engwall, M., Gallacher, D. J., Geys, H., et al. (2014). The concordance between nonclinical and phase I clinical cardiovascular assessment from a cross-company data sharing initiative. *Toxicological Sciences*, 142(2), 427–435.
- Extramiana, F., Maison-Blanche, P., Haggui, A., Badilini, F., Beaufils, P., & Leenhardt, A. (2006). Control of rapid heart rate changes for electrocardiographic analysis: Implications for thorough QT studies. *Clinical Cardiology*, 29, 534–539.
- Fermini, B., Hancox, J. C., Abi-Gerges, N., Bridgland-Taylor, M., Chaudhary, K. W., Colatsky, T., et al. (2016). A new perspective in the field of cardiac safety testing through the comprehensive in vitro proarrhythmia assay paradigm. *Journal of Biomolecular Screening*, 21(1), 1–11.
- Frommeyer, G., & Eckardt, L. (2016). Drug-induced proarrhythmia: Risk factors and electrophysiological mechanisms. *Nature Reviews Cardiology*, 13, 36–47.
- Funck-Brentano, C., Kibele, Y., Le Coz, F., Poirier, J. M., Mallet, A., & Jaillon, P. (1991). Rate dependence of sotalol-induced prolongation of ventricular repolarization during exercise in humans. *Circulation*, 83, 536–545.
- Gintant, G., Sager, P. T., & Stockbridge, N. (2016). Evolution of strategies to improve pre-clinical cardiac safety testing. *Nature Reviews Drug Discovery*. <http://dx.doi.org/10.1038/nrd.2015.34> (Published online 19 February 2016).
- Guo, D., Liu, Q., Liu, T., Elliott, G., Gings, M., et al. (2011). Electrophysiological properties of HBI-3000: A new antiarrhythmic agent with multiple-channel blocking properties in human ventricular myocytes. *Journal of Cardiovascular Pharmacology*, 57, 79–85.
- Holmes, A., Bonner, F., & Jones, D. (2015). Assessing drug safety in human tissues - What are the barriers? *Nature Reviews Drug Discovery*, 14(8), 585–587.
- Hondeghem, L. M. (2016). Disturbance of cardiac wavelength and repolarization precede torsade de pointes and ventricular fibrillation in Langendorff perfused rabbit hearts. *Progress in Biophysics and Molecular Biology*, 121(1), 3–10.
- Johannessen, L., Vicente, J., Mason, J. W., Sanabria, C., Waite-Labott, K., et al. (2014). Differentiating drug-induced multichannel block on the electrocardiogram: Randomized study of dofetilide, quinidine, ranolazine, and verapamil. *Clinical Pharmacology & Therapeutics*, 96(5), 549–558.
- Jost, N., Virág, L., Bitay, M., Takács, J., Lengyel, C., Biliczki, P., et al. (2005). Restricting excessive cardiac action potential and QT prolongation: A vital role for IKs in human ventricular muscle. *Circulation*, 112, 1392–1399.
- Jost, N., Virág, L., Comtois, P., Balázs, O., Szuts, V., Seprényi, G., et al. (2013). Ionic mechanisms limiting cardiac repolarization reserve in humans compared to dogs. *Journal of Physiology*, 591(17), 4189–4206.
- Lande, G., Maison-Blanche, P., Fayn, J., Ghanafar, M., Coumel, P., & Funck-Brentano, C. (1998). Dynamic analysis of dofetilide-induced changes in ventricular repolarization. *Clinical Pharmacology & Therapeutics*, 64(3), 312–321.
- Lawrence, C. L., Bridgland-Taylor, M. H., Pollard, C. E., Hammond, T. G., & Valentin, J. P. (2006). A rabbit Langendorff heart proarrhythmia model: Predictive value for clinical identification of torsades de pointes. *British Journal of Pharmacology*, 149, 845–860.
- McComb, J. M., McGovern, B., McGowan, J. B., Ruskin, J. M., & Garan, H. (1987). Electrophysiologic effects of d-sotalol in humans. *Journal of the American College of Cardiology*, 10(1), 211–217.
- Melicherik, J., Brachmann, J., Schöls, W., Hilbel, T., Beyer, T., et al. (1999). Rate and time dependent effects of d-sotalol on the monophasic action potential after sudden increase of the heart rate. *Pacing and Clinical Electrophysiology*, 22(1), 65–72.
- Mummery, C., Ward-van Oostwaard, D., Doevendans, P., Spijkier, R., van den Brink, S., Hassink, R., et al. (2003). Differentiation of human embryonic stem cells to cardiomyocytes: Role of coculture with visceral endoderm-like cells. *Circulation*, 107, 2733–2740.
- Näbauer, M., & Käb, S. (1998). Potassium channel down-regulation in heart failure. *Cardiovascular Research*, 37, 324–334.
- Näbauer, M., Beuckelmann, D. J., Überfuhr, P., & Steinbeck, G. (1996). Regional differences in current density and rate-dependent properties of the transient outward current in subepicardial and subendocardial myocytes of human left ventricle. *Circulation*, 93, 168–177.
- Nademanee, K., Stevenson, W. G., Weiss, J. N., Frame, V. B., Antimisariis, M. G., et al. (1990). Frequency-dependent effects of quinidine on the ventricular action potential and QRS duration in humans. *Circulation*, 81(3), 790–796.
- Nawrath, H., & Eckel, L. (1979). Electrophysiological study of human ventricular heart muscle treated with quinidine: Interaction with isoprenaline. *Journal of Cardiovascular Pharmacology*, 1(4), 415–425.
- O'Hara, T., Virág, L., Varró, A., & Rudy, Y. (2011). Simulation of the undiseased human cardiac ventricular action potential: Model formulation and experimental validation. *PLoS Computational Biology*, 7(5), e1002061.
- Okada, Y., Ogawa, S., Sadanaga, T., & Mitamura, H. (1996). Reverse use-dependent blocking actions of class III antiarrhythmic drugs by 24-hour Holter electrocardiography. *Journal of the American College of Cardiology*, 27(1), 84–89.
- Perel, P., Roberts, I., Sena, E., Wheble, P., Briscoe, C., Sandercock, P., et al. (2007). Comparison of treatment effects between animal experiments and clinical trials: Systematic review. *BMJ*, 334(7585), 197.
- Picini, J. P., Whellan, D. J., Berridge, B. R., Finkle, J. K., Pettit, S. D., Stockbridge, N., et al. (2009). Current challenges in the evaluation of cardiac safety during drug development: Translational medicine meets the critical path initiative. *American Heart Journal*, 158, 317–326.
- Polak, S., Pugsley, M. K., Stockbridge, N., Garnett, C., & Wiśniowska, B. (2015). Early drug discovery prediction of proarrhythmia potential and its covariates. *The AAPS Journal*, 17(4), 1025–1032.
- Qu, Y., & Vargas, H. M. (2015). Proarrhythmia risk assessment in human induced pluripotent stem cell-derived cardiomyocytes using the maestro MEA platform. *Toxicological Sciences*, 147(1), 286–295.
- Qu, Y., Gao, B., Fang, M., & Vargas, H. M. (2013). Human embryonic stem cell derived cardiac myocytes detect hERG-mediated repolarization effects, but not Nav1.5 induced depolarization delay. *Journal of Pharmacological and Toxicological Methods*, 68(1), 74–81.
- Redfern, W. S., Carlsson, L., Davis, A. S., Lynch, W. G., MacKenzie, I., et al. (2003). Relationships between preclinical cardiac electrophysiology, clinical QT interval prolongation and torsade de pointes for a broad range of drugs: Evidence for a provisional safety margin in drug development. *Cardiovascular Research*, 58, 32–45.
- Rosen, M. R. (2001). Isolated tissue models and proarrhythmia. *European Heart Journal*, 3(Suppl. K), K64–K69.
- Sager, P. T., Gintant, G., Turner, J. R., Pettit, S., & Stockbridge, N. (2014). Rechanneling the cardiac proarrhythmia safety paradigm: A meeting report from the cardiac safety research consortium. *American Heart Journal*, 167(3), 292–300.
- Sager, P. T., Uppal, P., Follmer, C., Antimisariis, M., Pruitt, C., & Singh, B. N. (1993). Frequency-dependent electrophysiologic effects of amiodarone in humans. *Circulation*, 88, 1063–1071.
- Scannell, J. W., Blanckley, A., Boldon, H., & Warrington, B. (2012). Diagnosing the decline in pharmaceutical R&D efficiency. *Nature Reviews Drug Discovery*, 11(3), 191–200.
- Scott, C. W., Peters, M. F., & Dragan, Y. P. (2013). Human induced pluripotent stem cells and their use in drug discovery for toxicity testing. *Toxicology Letters*, 219(1), 49–58.
- Seok, J., Warren, H. S., Cuenca, A. G., Mindrinos, M. N., Baker, H. V., Xu, W., et al. (2013). Genomic responses in mouse models poorly mimic human inflammatory diseases. *Proceedings of the National Academy of Sciences of the United States of America*, 110(9), 3507–3512.



- Shah, R. R. (2005). Drug-induced QT interval prolongation-regulatory guidance and perspectives on hERG channel studies. *Novartis Foundation Symposium*, 266, 251–285.
- Sivagangabalan, G., Nazzari, H., Bignolais, O., Maguy, A., Naud, P., Farid, T., et al. (2014). Regional ion channel gene expression heterogeneity and ventricular fibrillation dynamics in human hearts. *PLoS One*, 9(1), e82179.
- Stockbridge, N., Morganroth, J., Shah, R. R., & Garnett, C. (2013). Dealing with global safety issues: Was the response to QT-liability of non-cardiac drugs well-coordinated? *Drug Safety*, 36(3), 167–182.
- Vargas, H. M., Bass, A. S., Koerner, J., Matis-Mitchell, S., Pugsley, M. K., Skinner, M., et al. (2015). Evaluation of drug-induced QT interval prolongation in animal and human studies: A literature review of concordance. *British Journal of Pharmacology*, 172(16), 4002–4011.
- Vermeulen, J., McGuire, M. A., Ophof, T., Coronel, R., De Bakker, J. M. T., et al. (1994). Triggered activity and automaticity in ventricular trabeculae of failing human and rabbit hearts. *Cardiovascular Research*, 28(10), 1547–1554.
- Vicente, J., Johannesen, L., Masom, J. W., Crumb, W. J., Pueyo, E., et al. (2015). Comprehensive T wave morphology assessment in a randomized clinical study of dofetilide, quinidine, ranolazine, and verapamil. *Journal of the American Heart Association*, 4(4) (pii: e001615).
- Wettwer, E., Amos, G., Gath, J., Zerkowski, H. R., Reidemeister, J. C., & Ravens, U. (1993). Transient outward current in human and rat ventricular myocytes. *Cardiovascular Research*, 27(9), 1662–1669.
- Wettwer, E., Amos, G. J., Posival, H., & Ravens, U. (1994). Transient outward current in human ventricular myocytes of subepicardial and subendocardial origin. *Circulation Research*, 75, 473–482.
- Yuan, S., Wohlfart, B., Rasmussen, H. S., Olsson, S., & Blomström-Lundqvist, C. (1994). Effect of dofetilide on cardiac repolarization in patients with ventricular tachycardia. A study using simultaneous monophasic action potential recordings from two sites in the right ventricle. *European Heart Journal*, 15(4), 514–522.